Hindawi
Advances in Civil Engineering
Volume 2020, Article ID 2748092, 8 pages
https://doi.org/10.1155/2020/2748092

Research Article

The Evolution of Thermal Conductivity and Pore Structure for Coal under Liquid Nitrogen Soaking

Bo Li,[1,2,3] **Yongjie Ren**,[1] **and XiaoQuan Lv**[1]

[1]*School of Safety Science and Engineering, Henan Polytechnic University, Jiaozuo 454003, China*
[2]*Hebei State Key Laboratory of Mine Disaster Prevention, North China Institute of Science and Technology, Beijing 101601, China*
[3]*Collaborative Innovation Center of Coal Work Safety, Henan Province, Henan Polytechnic University, Jiaozuo 454003, China*

Correspondence should be addressed to Bo Li; anquanlibo@163.com

Received 18 September 2019; Revised 26 May 2020; Accepted 16 June 2020; Published 8 July 2020

Academic Editor: Xuemei Liu

An experimental system for liquid nitrogen soaking and real-time temperature measurement was designed and implemented to investigate the characteristics of temperature field changes in coal under liquid nitrogen soaking. Then, the heat conduction law of the coal in the process of liquid nitrogen soaking and room temperature recovery for dry and water-saturated coal were examined. The microstructure characteristics of the coal before and after liquid nitrogen soaking were analyzed with nuclear magnetic resonance (NMR) technology. The results showed that, during the liquid nitrogen cold soaking process, the heat transfer law of the dry and water-saturated coal samples exhibited a notable three-stage distribution. For the room temperature recovery process, the dry and water-saturated coal samples exhibited rapid heating characteristics, and the cooling rate gradually decreased to zero. NMR test results indicated that the liquid nitrogen soaking increased the number of micro and small pores in the coal. Thermal stress analysis revealed that the thermal stress generated by the dry coal was larger than that produced by the saturated coal, and the damage was primarily caused by thermal stress. However, the permeability of the saturated coal was better than that of the dry coal. The damage on the saturated coal was caused by the volume expansion of pores and fissures caused by water-ice phase transition.

1. Introduction

Given the serious shortage in water resources and the increase in environmental pollution, many scholars explored waterless fracturing as a new means of coal seam gas extraction. Liquid nitrogen was regarded as a potential water-free fracturing fluid due to its ultralow temperature [1–5]. Recently, some works were carried out to investigate the influence of low temperature on the pore structure and mechanical properties of coal [6, 7]. Cai et al. [8] evaluated the porosity of rock samples before and after freezing with liquid nitrogen by using nuclear magnetic resonance (NMR) and found that liquid nitrogen freezing can damage the pore structure of rocks, and the damage degree is influenced by lithology, porosity, and water saturation. Zhang et al. [9] used a laser microscope to observe the expansion of the primary fissure and new crack initiation in the coal samples before and after liquid nitrogen freezing and thus analyzed the expansion and mechanism of the primary fissure of coal samples on the basis of fracture mechanics theory. The mesoscopic damage mechanism of sandstone under uniaxial compression was evaluated by Ren and Hui [10] through a CT test, and CT images of crack initiation, development, macrocrack formation, and failure were obtained. They deemed that the original fissures of rocks play a significant role in the crack initiation and macroscopic damage of new cracks. Enayatpour et al. [11] conducted a theoretical analysis and reported that reducing the temperature of a reservoir rock produces thermal strain and tensile stress. However, in the field of coal reservoir, there are few studies on the changes of coal pore cracks caused by temperature impact.

The change in the pores and cracks of coal under low temperatures is the result of the coupling of multiple

physical fields [12–14], and the change in the temperature field during this coupling is a basic problem to be addressed [15]. In recent years, some scholars investigated the temperature field of coal under the effect of low temperatures. In frozen soil and cold zone engineering, several scholars have conducted a theoretical analysis and simulation calculation of temperature field. Lai et al. [16] simplified the heat conduction equation for a circular tunnel according to the actual conditions of a frozen soil area and obtained an approximate analytical solution for the freezing process of the tunnel. Du et al. [17] used the ANSYS software to simulate the tunnel temperature field numerically and solve the problem of tunnel disasters in cold regions. The researchers studied the distribution law of the tunnel temperature field in consideration of various practical factors and provided the theoretical basis for the insulation and antifreeze technology of cold tunnels. Chen et al. [18] determined frozen soil thermal parameters at different negative temperatures on the basis of the measured unfrozen water content in frozen soils. They used the ABAQUS software to obtain numerical values of the transient temperature field. By combining the finite element software and freezing experiments, Wang et al. [19] established the curve of temperature variation over time in the soil freezing process. They revealed the change law of the 3D temperature field of soil in an artificial freezing process.

It is generally believed that the temperature transfer in coal is affected by different influencing factors. Park et al. [20] investigated the relationship between the thermal-physical parameters of rock and temperature. The results showed that the specific heat and thermal expansion coefficient of rocks decrease with the depressing temperature in the range of −160°C–40°C. The coefficient of thermal conductivity varies only slightly with temperature. Mottaghy and Rath [21] studied the effect of latent heat of phase change on temperature. The migration of nonfrozen water and the concentration of solutes in water under porous conditions directly affect temperature transfer [22].

It is very difficult to determine the factors of coal temperature transfer at low temperatures through theoretical analysis and simulation calculation. Therefore, several scholars directly measured the variation law of the internal temperature field of coal by using preburied temperature measuring elements. Shen et al. [23] studied the internal heat transfer law of rocks in a freeze-thaw cycle, embedded a temperature sensor into a sandstone sample, and measured the temperature change at various points inside the sample. Zhou et al. [24] used a cryogenic thermostatic bath to provide the required ambient temperature for a soil sample. A temperature sensor was inserted into the center of the soil sample to monitor the sample's temperature in real time. The freezing and supercooling temperatures of the soil under different cooling conditions were also studied.

In summary, the previous studies focused on frozen soil, frozen rock, and other fields, and there are few studies on the temperature field and microstructure changes of coal under freezing. The freezing and melting law of coal under the impact of liquid nitrogen is the key to judge the state of coal and the evolution of pores and fractures. Therefore, this paper directly measures the temperature propagation law of coal under liquid nitrogen cold socking through experiment.

2. Methodology

2.1. Experimental System. A temperature propagation experiment was performed with liquid nitrogen cold soaking. An experimental system for liquid nitrogen cold freezing and real-time temperature measurement (Figure 1) was designed and implemented independently for the experiment. The experimental system was composed of a self-pressurized liquid nitrogen tank, thermal insulation container, coal sample clamping device, temperature sensor, and real-time temperature acquisition device. The coal sample clamping device had good thermal insulation. Its inner wall diameter was 50 mm, and the inner diameter of the bottom was slightly smaller than the coal sample diameter. The coal sample was placed in the clamping device. During the experiment, liquid nitrogen from the self-pressurized liquid nitrogen tank was continuously injected into the insulation container to ensure that the liquid nitrogen in the container is always in contact with the coal sample bottom.

2.2. Coal Sample Preparation. Anthracite coal samples were collected from Jiu Lishan Mine in Jiaozuo, China. Core drilling and core cutting machines in laboratory were utilized to process the coal samples into cylindrical samples with a diameter of 50 mm and a height of 100 mm. The prepared coal samples were placed in a constant-temperature drying box. The drying temperature was adjusted to 55°C, and the drying process was implemented. A borehole with a diameter of 4 mm was drilled vertically down the top center of a coal sample at a depth of 60 mm to measure the internal temperature. A temperature sensor was placed at the bottom of the hole. The prepared coal samples are shown in Figure 2.

2.3. Experimental Procedure. Given the special nature of liquid nitrogen, the heat transfer law was investigated through liquid nitrogen cold leaching. This work also considered the cold immersion of liquid nitrogen and the bottom contact of the coal sample. Therefore, a liquid nitrogen cold immersion system was designed and implemented. Coal samples in dry and water-saturated conditions were selected for testing. The experimental environment had a room temperature of 23°C. The experimental procedures were as follows:

(1) A coal sample was placed in the experimental device, and the acquisition time interval of the temperature acquisition software was set to 1 min.

(2) The self-pressurized liquid nitrogen tank was opened, and liquid nitrogen was injected into the heat-preservation container until the liquid nitrogen submerged to the bottom surface of the coal sample.

(3) The self-pressurized liquid nitrogen tank valve was adjusted to ensure that the liquid nitrogen in the

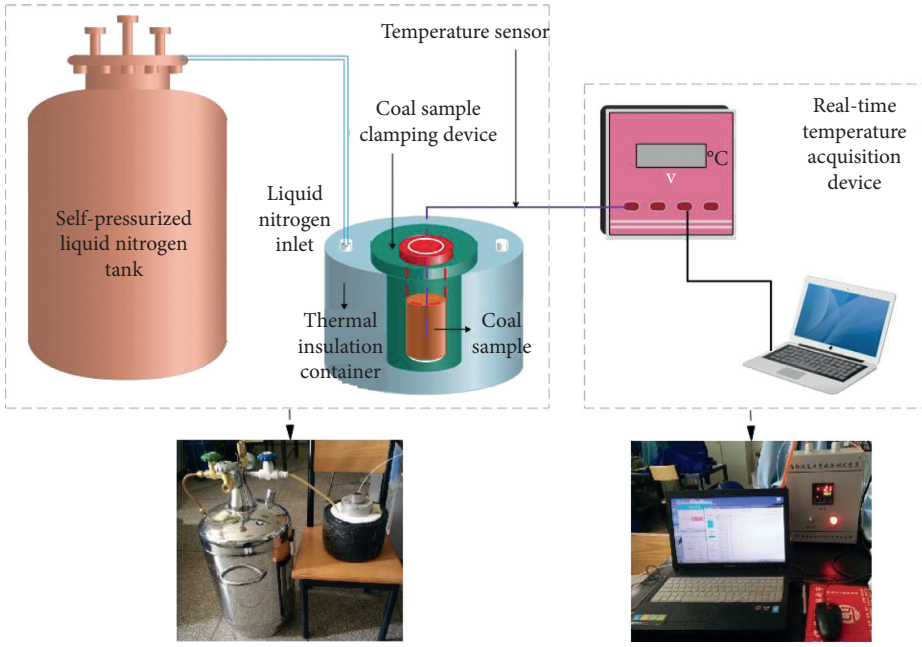

Figure 1: Experimental system for liquid nitrogen freezing and real-time temperature measurement.

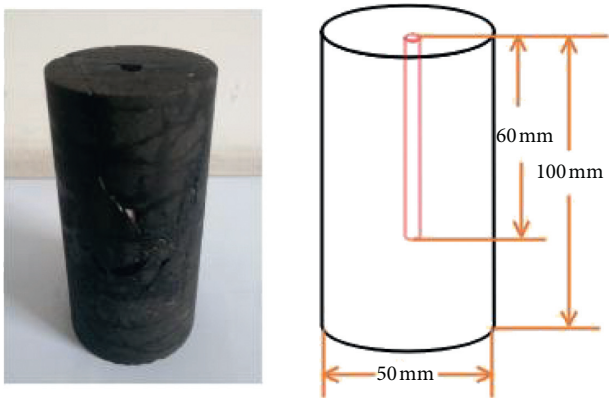

Figure 2: Coal samples for testing.

heat-preservation container was inundated at the bottom surface of the coal sample.

(4) When the temperature change was less than 2°C within 30 min, the liquid nitrogen cold soak test was considered to be finished. The coal sample was extracted from the coal sample holding device and placed in a room-temperature environment. The temperature changes were continuously recorded.

(5) The experiment was repeated for the subsequent coal samples.

3. Results and Analysis

3.1. Theoretical Analysis of Heat Conduction of Coal under Liquid Nitrogen Soaking. The heat transfer process of dry coal during freezing under the action of liquid nitrogen belongs to single-phase medium heat transfer, without considering water seepage and phase change. According to the basic Fourier heat transfer law [25], the relationship between heat flux and temperature gradient is

$$q + \lambda \nabla \theta = 0, \tag{1}$$

where q is the heat flux, J/s; λ is the Fourier thermal conductivity; and θ is the object temperature, °C.

According to the law of conservation of energy,

$$\rho C \frac{\partial \theta}{\partial t} + \nabla q = Q, \tag{2}$$

where ρ is density, kg/m^3; C is specific heat capacity, J/(kg·°C); Q is heat source; and t is time, s.

By combining formula (1) and formula (2), we can get

$$\rho C \frac{\partial \theta}{\partial t} - \nabla \lambda \nabla \theta = Q. \tag{3}$$

This equation reflects the law of temperature change in coal under dry state.

For the saturated coal undergoing water ice phase change, its temperature field can be divided into three regions: solid phase region, liquid region, and water ice phase transition region. The change of thermophysical parameters in the process of phase change of coal material itself is not considered, as only the effect of saturated pore water ice phase change is considered; then the detailed description is as follows [23]:

(1) For the solid phase region, the water in the pore is completely frozen; the equation of heat conduction can be expressed as

$$\frac{1}{r}\frac{\partial}{\partial r}\left(r\frac{\partial T_s}{\partial r}\right) = \frac{1}{\alpha_s}\frac{\partial T_s}{\partial t}, \quad 0 < r < r_s(t), t > 0, \tag{4}$$

where T_s is the temperature at a certain point in the solid phase region; $r_s(t)$ is the radius of the solid phase

region, mm; α_s is the mixed diffusion coefficient of solid phase, $m^2 \cdot s$. The mixed diffusion coefficient of solid phase α_s can be expressed:

$$\alpha_s = \frac{k_s}{(\rho_s c_s)} = \frac{(1-n)k_r}{(\rho_r c_r)} + \frac{nk_i}{(\rho_i c_i)}, \quad (5)$$

where the subscripts s, r, and i represent the solid phase, coal, and ice, respectively; k, ρ, and c are the thermal conductivity (w/(m·K)), density (kg/m^3), and specific heat capacity (kJ/(kg·K)), respectively. n is the coal porosity.

(2) The heat conduction equation in the liquid region is expressed as follows:

$$\frac{1}{r}\frac{\partial}{\partial r}\left(r\frac{\partial T_l}{\partial r}\right) = \frac{1}{\alpha_l}\frac{\partial T_l}{\partial t}, \quad r_l(t) < r < R, t > 0, \quad (6)$$

where T_l is the temperature of a point in the liquid phase region; $r_l(t)$ is the radius of the liquid phase region, mm; α_l is the mixing diffusion coefficient in the liquid phase region, m^2/s, which is determined by the following formula:

$$\alpha_l = \frac{k_l}{(\rho_l c_l)} = \frac{(1-n)k_r}{(\rho_r c_r)} + \frac{nk_w}{(\rho_w c_w)}, \quad (7)$$

where the subscripts l and w represent liquid and water, respectively.

(3) For the water ice phase transition region, it is in the two-phase change region. Influenced by the latent heat of phase transition, its heat conduction equation shows the following characteristics:

$$\frac{1}{r}\frac{\partial}{\partial r}\left(r\frac{\partial T_{sl}}{\partial r}\right) + \frac{\rho_{sl}}{k_{sl}}\Delta h n\frac{df_s}{dt} = \frac{1}{\alpha_{sl}}\frac{\partial T_{sl}}{\partial t}, \quad r_s(t) < r < r_l(t), t > 0, \quad (8)$$

where T_{sl} is the temperature at a certain point in the transformation region; Δh is the latent heat of water ice transformation region, kJ/(kg·K); f_s is the ice content at a certain time, %.

α_{sl} is the mixed diffusion coefficient (m^2/s) in the phase transformation region, which is determined by the following formula:

$$\alpha_{sl} = \frac{k_{sl}}{(\rho_{sl} c_{sl})}, \quad (9)$$

where the subscript sl represents water ice transformation region.

3.2. Temperature Measurement Test Results. In accordance with the experimental scheme, the temperature variation at the temperature measurement point in the entire process of liquid nitrogen cold soaking and room temperature recovery was evaluated. The following rules were obtained from the experimental results in Figure 3.

(1) In the liquid nitrogen cold soaking process, the heat transfer law of the dry and saturated coal samples had a three-stage distribution. The cooling rate in the first stage gradually increased from zero. After a certain degree, the temperature changed linearly over time in the second stage. The cooling rate in the third stage gradually decreased until the temperature stabilized.

(2) In the liquid nitrogen cold soaking process, the temperature change in the saturated coal sample was relatively slow, and the total heat conduction balance was experienced for a long period. The dry coal sample reached temperature balance approximately 1 hour earlier than the saturated coal sample did. The details of the time changes in each stage are shown in Table 1. Notably, the temperature at which the dried coal sample reached equilibrium was the liquid nitrogen temperature (−196°C). The saturated coal sample reached equilibrium within −186°C to −188°C, and the temperature continuously fluctuated within this range.

(3) In the room temperature recovery process, the dry and saturated coal samples exhibited rapid temperature rise characteristics, and the cooling rate gradually decreased.

(4) In the room temperature recovery process, the temperature of the saturated coal sample changed slowly. The saturated coal sample rapidly warmed to 16.5°C in 95 min, and the dried coal sample rapidly warmed to 21.1°C in 80 min. Then, the temperature gradually increased. The temperature at which the dried coal sample reached equilibrium was room temperature (23°C), whereas the equilibrium temperature of the saturated coal sample was lower than the ambient temperature.

The experimental data indicated that the temperature change law of the dry and saturated coal samples during liquid nitrogen cold leaching exhibited a certain degree of difference, which was mainly reflected in the liquid nitrogen cold leaching process or room temperature recovery process. The temperature changes were relatively slow; hence, the total amount of time for the temperature to reach equilibrium was large. Under the same experimental conditions, this experimental phenomenon can be viewed as being related to the latent heat of ice release from the saturated coal samples.

During the freezing process of water, the hydrogen bonds of water molecules gradually shrink, the Coulomb force decreases, and the length shortens. With the deepening of the freezing process, the hydrogen bonds in the water molecules are gradually saturated; finally, a neat hexagonal crystal lattice appears, which marks the completion of the water and phase transformation process.

In the process of coal temperature rising and melting with the room temperature environment, the unstable hydrogen bond of water molecules increases gradually under the interference of external heat source, the Coulomb

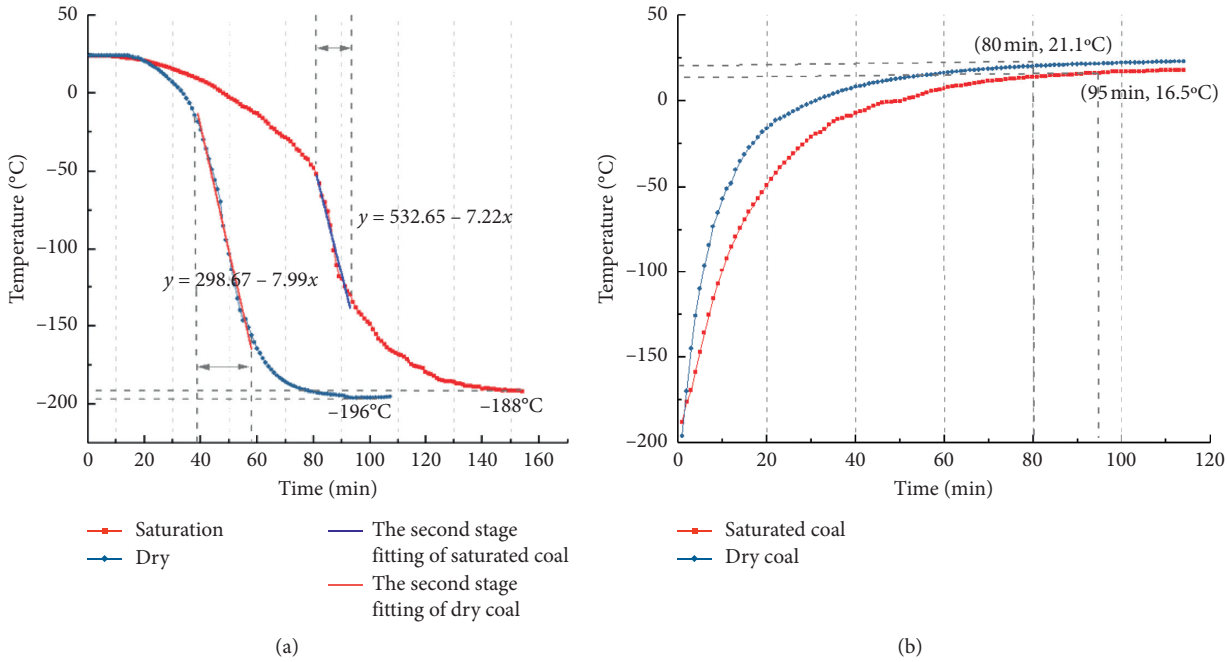

Figure 3: Change in the internal temperature of the coal samples. (a) Liquid nitrogen cold soaking process. (b) Room temperature recovery process.

Table 1: Freezing time of coal samples at different temperature levels.

Coal samples	Liquid nitrogen cold soaking time (min)			
	First stage	Second stage	Third stage	Total time
Dry	38	19	35	92
Saturation	80	12	58	150

repulsion force increases gradually, the length of hydrogen bond becomes longer, and the molecules of each unit gradually become active and even present the free state again. Along with this process is a series of exothermic processes, and finally the unstable water molecules present with complete free state or very short hydrogen bond combination, which marks the completion of melting process The phase transition process of ice water is over, as the ice in the coal gradually melted, the humidity around the built-in temperature sensor of the saturated coal increased, the absolute humidity in the air decreased, and additional heat was absorbed to form a wet and dry ball. The difference in temperature [26] showed that the equilibrium temperature of the dry and saturated coal varied by 3°C to 4°C.

During the liquid nitrogen cold soaking, the crack extension in the samples showed a direct relationship to heat transfer. In in situ formations, factors such as in situ stress, frost-heaving force, shrinkage stress of matrix particles, and high-pressure nitrogen affect the deformation of the samples and crack extension. When the internal stress on matrix particles exceeds or equals the tensile strength of particles in coal masses, new cracks are generated; otherwise, cracks are not generated.

3.3. Influence of Low Temperature on the Pore Structure of Coal. To compare and analyze the pore change characteristics of coal samples before and after treatment, we used the dry and saturated coal samples for the examination of the temperature propagation law of liquid nitrogen cold immersion and room temperature recovery. The pore distribution of the coal samples was tested through an NMR test. In addition, the correlation between temperature propagation and pore change was explored. The overall experimental process is shown in Figure 4. The NMR equipment used was a MicroMR12-025V low-field NMR analyzer. The main technical parameters of the equipment are as follows: magnet uniformity of 20 ppm, magnetic field strength of 0.24 T, pulsed radio frequency of 1–60 MHz, and probe inner diameter of 38 mm.

The principle of NMR is known [27]. NMR technology was used in this work to detect fluid in the pores of coal. The NMR parameter T_2 spectrum area was employed to measure the volume of water when a coal sample was in a saturated state. Then, relaxation time T_2 indirectly reflected the pore size of the coal. The larger the T_2 value is, the larger the corresponding pore is.

The pore morphology of coal varies greatly, and different pore morphology corresponds to different pore

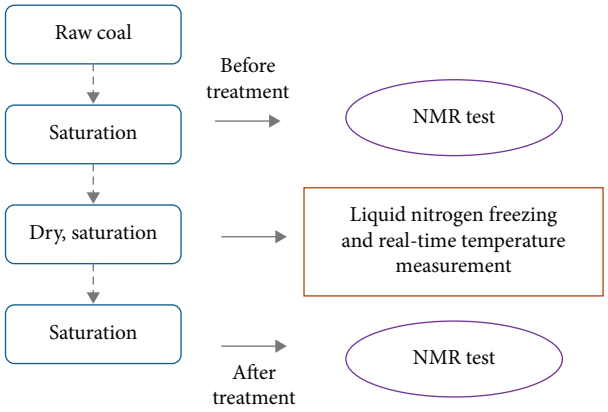

Figure 4: Experimental flow chart.

specific surface area. There is a certain positive correlation between the pore radius of coal and the pore throat radius:

$$\frac{1}{T_2} = \rho_2\left(\frac{f}{r}\right), \tag{10}$$

where T_2 is the lateral relaxation time of the pore fluid; ρ_2 is the relaxation intensity of the lateral surface; r is related to the shape of the pore; for the spherical pores, it represents the radius of the pore. f is the pore shape factor; for the coal structure, it generally takes a value of 2.

According to knowledge about nuclear magnetic resonance, the T_2 value reflects the size of coal pores. The larger the T_2 value, the larger the corresponding coal pores. The first peak T_2 relaxation time is 0.1 ~ 10 ms, converted to a pore size of about 1 ~ 100 nm, mainly including micropores and small pores, so it is called smaller pores; the second peak T_2 relaxation time is mainly 10 ~ 1,000 ms, converted into a pore size of about 100 ~ 10,000 nm, mainly including medium and large pores, so it is called larger pores; for the third peak, it corresponds to the fissure pores in the coal.

As shown in Figure 5, the first peak of the coal sample used in the experiment had a large spectrum area, and the micropores were well developed and compact. The effect of liquid nitrogen on the coal increased the number of small and micropores. Under the condition of coal sample saturation, the antipenetration effect on the coal was evident. As shown in Table 2, the first peak spectral area of the saturated coal sample increased by 101.8%. Its increase was 5.8 times that of the dried coal sample. Meanwhile, the increase in the second peak area was 83.1%, which is 22.5 times that of the dry coal sample. In the dry coal sample, the proportion of micropores decreased from 95.99% to 95.91%, whereas the proportion of small and medium-large holes increased. The coal sample with full water showed the opposite condition. That is, the effect of liquid nitrogen cold leaching on the pores of the dry and water-saturated coal samples was different, and the mechanism of action was different as well.

Stress constraints were imposed between the mineral particles after the coal was subjected to temperature shock. The stress at the boundary of a particle reached the limit of coal

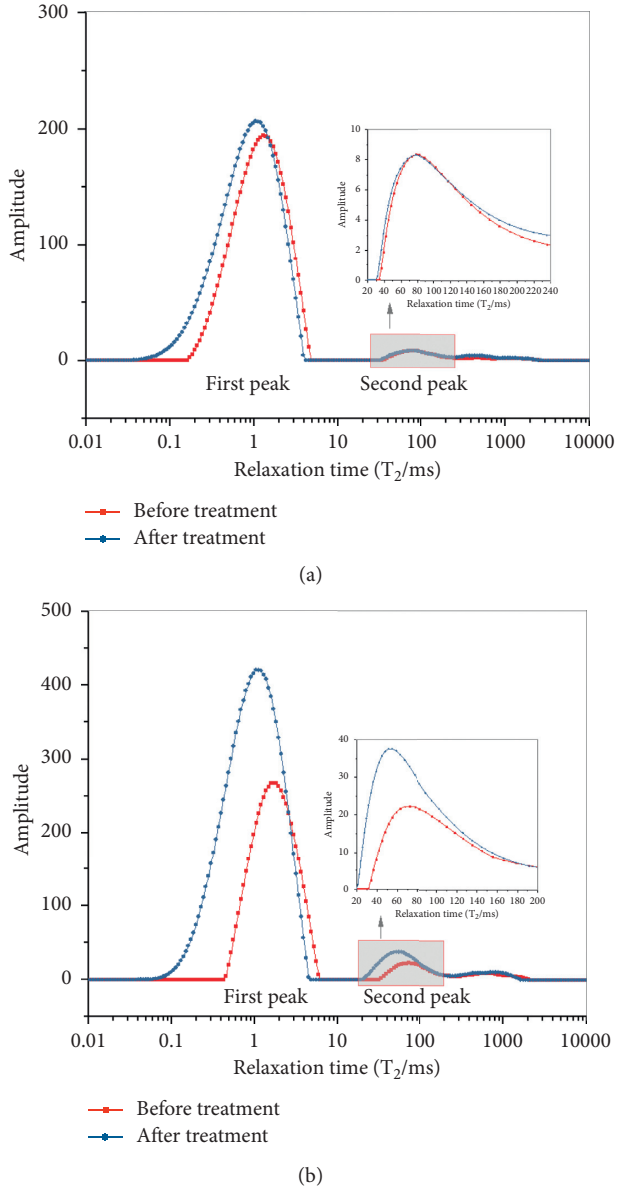

Figure 5: NMR T2 distribution. (a) Dry coal sample. (b) Saturated coal sample.

strength, resulting in new cracks. As the temperature gradient increased, the pores and cracks gradually expanded to produce macroscopic fractures [28]. The thermal stress due to temperature effects was calculated with the following equation [29]:

$$\sigma = \alpha\delta E\Delta T, \tag{11}$$

where σ represents thermal stress, α is the linear expansion coefficient of the coal, δ represents the Kronecker symbol (the value is here), E represents the coal elastic modulus, and ΔT denotes the temperature change.

An experiment was then performed on the temperature equilibrium law of liquid nitrogen cold immersion and room temperature recovery. The δ results showed that the temperature change in the dry coal sample, ΔT_d, was greater than that in the water-saturated coal sample, ΔT_w. The

Table 2: NMR spectrum integral area change.

Coal sample		Crest ratio (%)		Spectral integration area		Spectral integration area (%)
		Before treatment	After treatment	Before treatment	After treatment	
Dry	First peak	95.99	95.91	5142.99	6049.09	17.6
	Second peak	2.99	2.63	159.94	165.85	3.7
Saturation	First peak	91.18	92.74	6037.05	12181.25	101.8
	Second peak	6.13	5.66	405.85	743.13	83.1

physical parameters of both coal samples were the same; however, the thermal stress generated in the dry coal was greater than that in the saturated coal. The damage on the dry coal was due to the fracture of mineral particles caused by thermal stress. The damage on the saturated coal was caused by the pores and cracks that resulted from phase change.

4. Conclusions

(1) The experimental results for the heat transfer showed that the temperature variation in the coal during liquid nitrogen cold leaching had a three-stage distribution, and the cooling rate of the coal changed from high to low. After maintaining the maximum temperature drop rate for a certain period, the temperature gradually decreased and eventually stabilized. During the entire room temperature recovery process of the coal, the dry and saturated coal samples showed rapid heating characteristics, and the cooling rate decreased gradually.

(2) Given that the water phase in the coal was the latent heat release from ice, the rapid cooling stage (second stage) of the saturated coal during the liquid nitrogen cold immersion process lasted for a short time. In the process of liquid nitrogen soaking and room temperature recovery, the temperature change of saturated coal is generally slower than that of dry coal, and the total time of temperature reaching equilibrium is longer.

(3) The results of the NMR test showed that liquid nitrogen cold leaching increased the number of small and micropores inside the coal body of the coal. The effect on the coal was good under the water-saturated condition. Thermal stress was also analyzed. The dry coal had higher thermal stress than the saturated one. The damage was due to the thermal stress caused by the fracture between mineral particles, whereas the damage on the saturated coal was caused by phase change.

Data Availability

The data used to support the findings of this study are included within the article.

Conflicts of Interest

The authors declare that they have no conflicts of interest.

Acknowledgments

The authors would like to acknowledge the financial support from the National Natural Science Foundation for Young Scientists of China (51604096, 51874125, 51604116, 51704099, and 51574112), Hebei State Key Laboratory of Mine Disaster Prevention (KJZH2017K08), Young Key Teachers from Henan Polytechnic University (2019XQG-10), Young Talent Lift Project of Henan Province in 2020 (2020HYTP020), Natural Science Foundation of Hebei Province (E2016508036), Basic and Frontier Technology Research Project of Henan Province in 2016 (162300410031), Doctoral Fund of Henan Polytechnic University (B2015-05), and Open Fund of Energy Platform Laboratory Project (G201609).

References

[1] Y. P. Zhang, *Study on Liquid Nitrogen Fracturing Technology in CBM Wells*, Southwest Petroleum University, Chengdu, China, 2015, in Chinese.

[2] S. R. Ren, Z. K. Fan, L. Zhang, Y. Yang, J. Luo, and H. Che, "Mechanisms and experimental study of thermal-shock effect on coal-rock using liquid nitrogen," *Chinese Journal of Rock Mechanics and Engineering*, vol. 32, no. S2, pp. 3790–3794, 2013, in Chinese.

[3] M. Cha, X. Yin, T. Kneafsey et al., "Cryogenic fracturing for reservoir stimulation - laboratory studies," *Journal of Petroleum Science and Engineering*, vol. 124, pp. 436–450, 2014.

[4] L. Qin, C. Zhai, S. Liu, J. Xu, G. Yu, and Y. Sun, "Changes in the petrophysical properties of coal subjected to liquid nitrogen freeze-thaw - a nuclear magnetic resonance investigation," *Fuel*, vol. 194, pp. 102–114, 2017.

[5] C. Park, D. S. Cheon, J. H. Synn et al., "Experimental study on thermal and mechanical characteristics of rock at low temperature," in *Proceedings of International Symposium of the International Society for Rock Mechanics-Eurock 2005*, International Society for Rock Mechanics, Lisbon, Portugal, 2005.

[6] G. S. Yang, Y. B. Pu, and W. Ma, "Discussion on the damage propagation for the rock under the frost and thaw condition of frigid zone," *Journal of Experimental Mechanics*, vol. 17, no. 2, pp. 220–226, 2002, in Chinese.

[7] K. Kim, J. Kemeny, and M. Nickerson, "Effect of rapid thermal cooling on mechanical rock properties," *Rock Mechanics and Rock Engineering*, vol. 47, no. 6, pp. 2005–2019, 2014.

[8] C. Z. Cai, G. S. Yang, Z. W. Huang et al., "Experiment study of rock porous structure damage under cryogenic nitrogen freezing," *Rock and Soil Mechanics*, vol. 35, no. 4, pp. 965–971, 2014, in Chinese.

[9] C. H. Zhang, W. L. Li, X. Z. Wang et al., "Research of fracturing mechanism of coal subjected to liquid nitrogen cooling," *Journal of Hebei University of Science and Technology*, vol. 36, no. 4, pp. 425–430, 2015, in Chinese.

[10] J. X. Ren and X. T. Hui, "Primary study on meso-damage propagation mechanism of cracked-sandstone using computerized tomography under uniaxial compression," *Rock and Soil Mechanics*, no. S1, pp. 52–56, 2005, in Chinese.

[11] S. Enayatpour, E. V. Oort, and T. Patzek, "Freezefrac improves the productivity of gas shales," in *Proceedings of SPE Annual Technical Conference and Exhibition*, New Orleans, LA, USA, 2013.

[12] X. J. Tan, W. Z. Chen, G. J. Wu, and P. Zheng, "Study of thermo-hydro-mechanical-damage (THMD) coupled model in the condition of freeze-thaw cycles and its application to cold region tunnels," *Chinese Journal of Rock Mechanics and Engineering*, vol. 32, no. 2, pp. 239–250, 2013, in Chinese.

[13] J. R. Ma and G. S. Yang, "Study on liquid-thermal-stress coupling of freezing-thawing damage of soft rock," *Chinese Journal of Rock Mechanics and Engineering*, vol. 25, no. z1, pp. 4373–4377, 2004, in Chinese.

[14] S. B. Huang, Q. S. Liu, A. P. Cheng, and Y. Liu, "A coupled hydro-thermal model of fractured rock mass under low temperature and its numerical analysis," *Rock and Soil Mechanics*, vol. 39, no. 2, pp. 735–744, 2018, in Chinese.

[15] S. H. Xu, N. Li, G. G. Xu et al., "Thermal transfer and heat balance of saturated rock under freezing-thawing environment," *Chinese Journal of Rock Mechanics and Engineering*, vol. 35, no. 11, pp. 2225–2236, 2016, in Chinese.

[16] Y. M. Lai, W. B. Yu, Z. W. Wu et al., "Analytical solution of temperature field of circular section tunnel in cold region," *Journal of Glaciology and Geocryology*, vol. 23, no. 2, pp. 126–130, 2001, in Chinese.

[17] Y. H. Du, X. H. Yang, and C. G. Yan, "Numerical analysis of temperature field in seasonally cold zone tunnel," *Journal of Glaciology and Geocryology*, vol. 39, no. 2, pp. 366–374, 2017, in Chinese.

[18] Z. X. Chen, S. Q. Li, J. H. Xia, X.-C. Zhang, and C. Gui, "Calculation of frozen soil thermal parameters considering unfrozen water content," *Rock and Soil Mechanics*, vol. 38, no. S2, pp. 67–74, 2017, in Chinese.

[19] K. Wang, S. Q. Li, and J. H. Xia, "Temperature field of soil during freezing process," *Soil and Foundation Engineering*, no. 1, pp. 80–84, 2017, in Chinese.

[20] C. Park, J. H. Synn, H. S. Shin, D. S. Cheon, H. D. Lim, and S. W. Jeon, "An experimental study on the thermal characteristics of rock at low temperatures," *International Journal of Rock Mechanics and Mining Sciences*, vol. 41, no. 3, pp. 367-368, 2004.

[21] D. Mottaghy and V. Rath, "Latent heat effects in subsurface heat transport modelling and their impact on palaeotemperature reconstructions," *Geophysical Journal International*, vol. 164, no. 1, pp. 236–245, 2006.

[22] K. Watanabe and M. Mizoguchi, "Amount of unfrozen water in frozen porous media saturated with solution," *Cold Regions Science and Technology*, vol. 34, no. 2, pp. 103–110, 2002.

[23] Y. J. Shen, G. S. Yang, M. Wang et al., "Experimental and theoretical study on thermal conductivity of rock under cyclic freezing and thawing," *Chinese Journal of Rock Mechanics and Engineering*, vol. 35, no. 12, pp. 2417–2425, 2016, in Chinese.

[24] J. Z. Zhou, L. Tan, C. F. Wei, and H. Wei, "Experimental research on freezing temperature and super-cooling temperature of soil," *Rock and Soil Mechanics*, vol. 36, no. 3, pp. 777–785, 2015, in Chinese.

[25] H. P. HU, *Heat Conduction Theory*, pp. 1-2, University of Science and Technology of China Press, Hefei, China, 2010, in Chinese.

[26] W. James and Jabara, "Comparison of the wet bulb globe temperature and a modified botsball thermometer in an outdoor environment," *Applied Industrial Hygiene*, vol. 3, no. 11, pp. 303–309, 1988.

[27] J. L. Li, *Experimental Study on Deterioration Mechanism of Rock under the Conditions of Freezing-Thawing Cycles in Cold Regions Based on NMR Technology*, Central South University, Changsha, China, 2012, in Chinese.

[28] J. P. Wei, L. T. Sun, D. K. Wang, B. Li, M. Peng, and S. Liu, "Change law of permeability of coal under temperature impact and the mechanism of increasing permeability," *Journal of China Coal Society*, vol. 42, no. 8, pp. 1919–1925, 2017, in Chinese.

[29] J. Kang, *Research and Application of Rock Thermal Cracking*, Dalian University of Technology Press, Dalian, China, 2008, in Chinese.